

Supplement of Atmos. Chem. Phys., 20, 7359–7372, 2020
<https://doi.org/10.5194/acp-20-7359-2020-supplement>
© Author(s) 2020. This work is distributed under
the Creative Commons Attribution 4.0 License.



Supplement of

Enhanced growth rate of atmospheric particles from sulfuric acid

Dominik Stolzenburg et al.

Correspondence to: Paul M. Winkler (paul.winkler@univie.ac.at)

The copyright of individual parts of the supplement might differ from the CC BY 4.0 License.

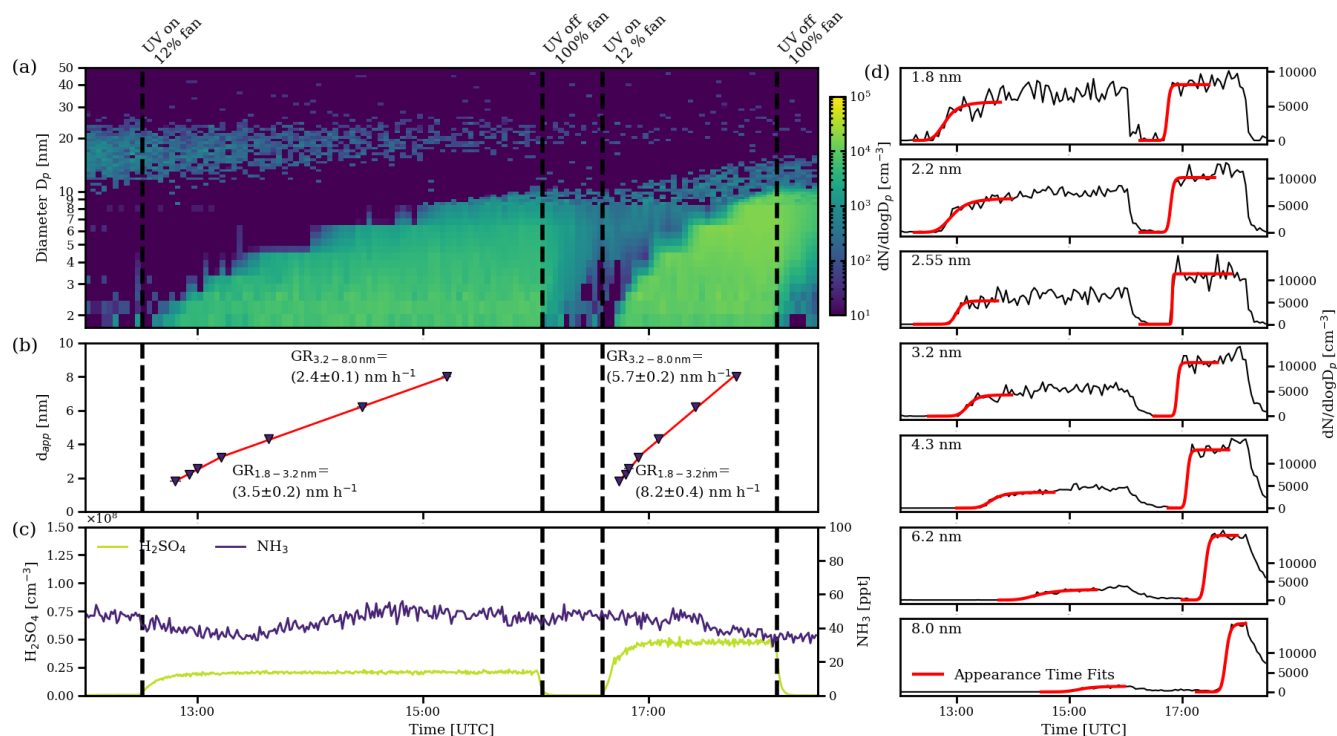


Figure S1: Typical set of experiments at 5 °C and 60 % relative humidity. (a) shows the combined particle number size distribution measured with a DMA-train from 1.8-8 nm and above 8 nm with a TSI nano-SMPS. (b) shows the 50% appearance time of each channel measured at diameter d_{app} in the DMA-train (blue triangles), and the corresponding linear fits in two size intervals, 1.8-3.2 nm and 3.2-8.0 nm. (c) shows the simultaneously measured traces of sulphuric acid (yellow line) and ammonia (blue line). Sulphuric acid is produced by reaction with $\text{OH}\cdot$ radicals, which are formed by UV illumination of the chamber. Different light intensities yield different levels of sulphuric acid, which in turn, yield different particle formation and growth rates. With increasing sulphuric acid concentrations, not only the particle concentrations get higher but also growth gets faster. This is clearly visible by looking at the leading edge of the growing population, which can be identified due to short cleaning stages in between the experiments, where wall losses are increased due to increasing fan speed and lights are turned off. (d) shows the time series of the individual channels of the DMA-train at the fixed sizes (1.8-8 nm) during the same experiments (black solid lines), together with the sigmoidal shaped appearance time fits to the data (red solid lines), which determine the 50% appearance times shown in (b).

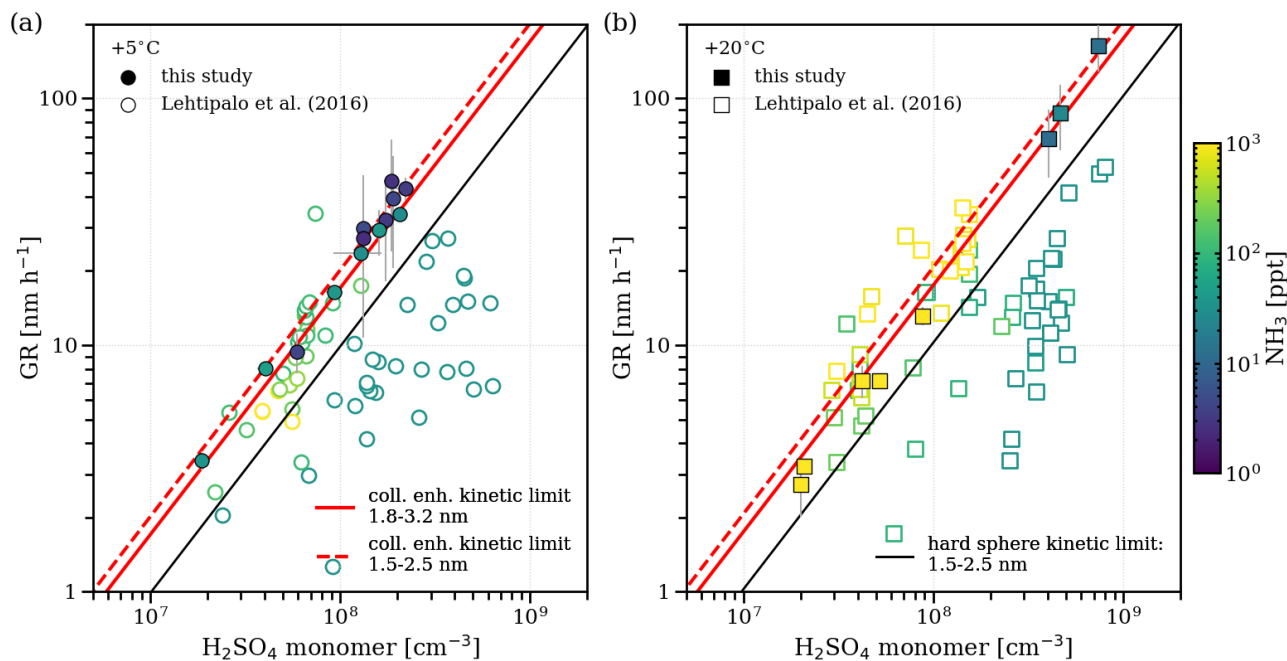


Figure S2: Comparison of the results from this study (filled symbols) with Lehtipalo et al. (2016) (open symbols) for two temperatures (a) 5 °C and (b) 20 °C. As the size range of the earlier study was smaller (1.5-2.5 nm mobility diameter), results with low NH_3 concentrations are considerably lower than the geometric limit of kinetic condensation (solid black line) due to evaporation of sulphuric acid. As soon as ammonia is present in significant amounts, the earlier results agree with the expected enhanced kinetic limit of condensation inferred in this study (dashed red line for 1.5-2.5 nm mobility diameter), also significantly above the geometric kinetic limit of condensation (Nieminen et al., 2010). The enhanced limit corresponding to the size range of the DMA-train measurements is also shown (red solid line 1.8-3.2 nm mobility diameter). The ammonia measurements significantly improved between the two studies and hence the lowest ammonia levels of the previous study are at the limit of detection of 35 ppt (blue-green points) and the true value could be considerably lower.

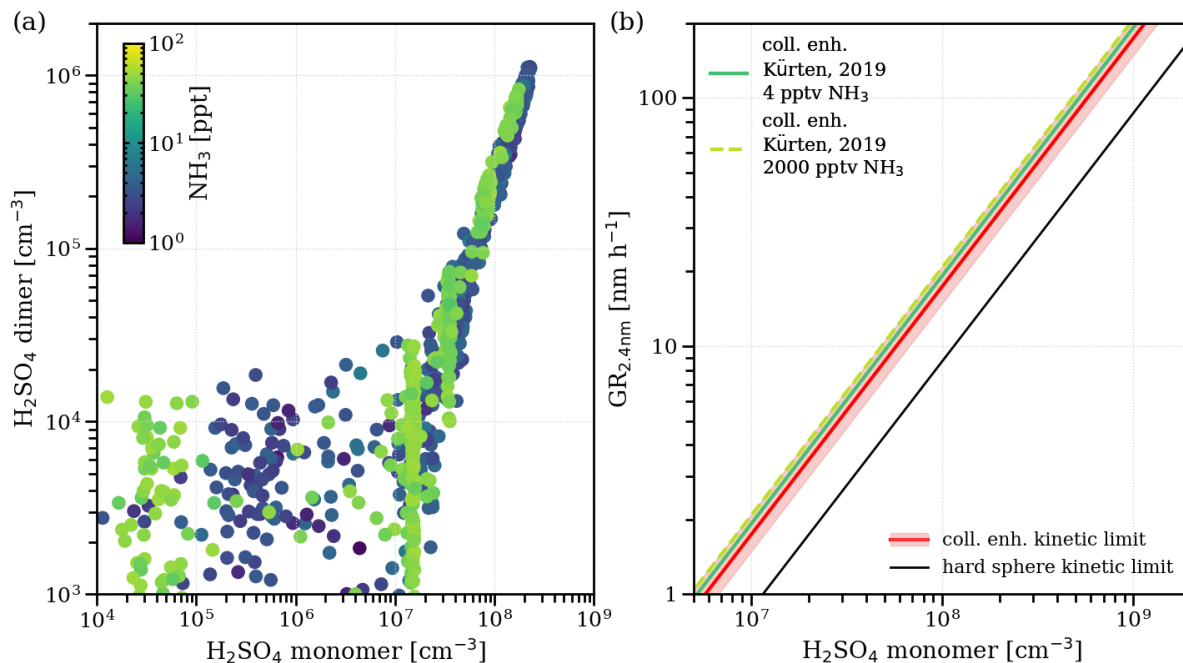


Figure S3: The cluster contribution to growth. Sulphuric acid, which is contained in small molecular clusters and hence is unaccounted in the measured monomer concentration could potentially contribute to growth by cluster condensation. This effect of ‘hidden’ sulphuric acid (Lehtipalo et al., 2016) would impact our kinetic results. (a) shows the measured ratio of H₂SO₄ monomers and dimers during growth experiments at 278.15 K with varying ammonia concentrations. While absolute cluster concentrations measured with the nitrate CI-API-ToF are subject to larger uncertainties for the H₂SO₄ dimer, the constant monomer/dimer ratio with and without addition of ammonia is indicating a negligible clustering effect. (b) shows a comparison of the growth rate predictions at the kinetic limit of condensation for three different approaches at a diameter of 2.4 nm and 278.15 K versus sulphuric acid monomer concentration. The black dashed line shows the geometric limit of kinetic condensation based on a hard-sphere assumption (Nieminen et al., 2010). The red line and red area show the result of this study (assuming $A = 4.6 \cdot 10^{-20}$ J and the naïve assumption on vapour and particle hydration) and its systematic uncertainty. The light green line and the dark green dashed line show the predictions of a model which includes sulphuric acid/ammonia clustering and evaporation (Kürten, 2019), for 4 pptv and 2000 pptv ammonia at 278.15 K (and assumed sulphuric acid density of $\rho=1.615$ g cm⁻³), respectively. An additional clustering and therefore cluster contribution to growth at higher ammonia levels is not significant in the model.

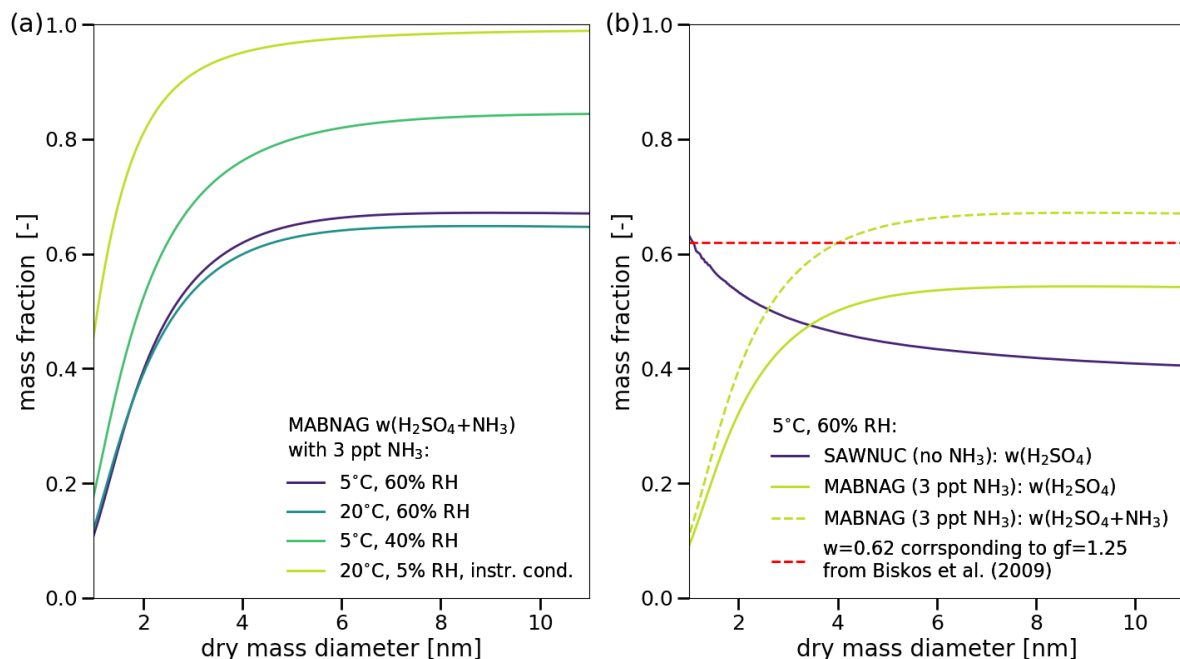


Figure S4: Modelled particle composition data from MABNAG and SAWNUC (Ehrhart et al., 2016). (a) shows the prediction from MABNAG for all temperatures and relative humidity values of this study including the instrument conditions (for the DMA-train) of 293.15 K and 5% relative humidity. Calculations are done for 3 pptv ammonia, but higher ammonia levels do not significantly change the composition. The combined sulphuric acid and ammonia mass fractions are used to estimate the hygroscopic growth factor according to Eq. (13). In that case, the error by using the density of sulphuric acid water solutions and neglecting ammonia is less than 20%. (b) shows a comparison of MABNAG and SAWNUC for the experiments at 278.15 K and 60% relative humidity. While SAWNUC predicts a decreasing sulphuric acid mass fraction with size, MABNAG shows the opposite trend. For the larger sizes, closer to bulk properties, MABNAG predicts a lower water content of the particles. For particles smaller than 2.5 nm, SAWNUC includes cluster simulations in order to predict the most probable water content, while MABNAG is based on bulk thermodynamics, explaining the difference. Hence, while MABNAG might overestimate the hydration at small sizes, SAWNUC might underestimate the hydration at larger sizes as the growing particles are partly neutralized by ammonia even at background ammonia concentrations. Taking the hygroscopic growth factor of 1.25 from Biskos et al. (2009) and assuming a completely dry measurement, the sulphuric acid mass fraction is 0.62, which is close to the cluster predictions of SAWNUC and the bulk predictions of MABNAG suggesting that the simplified assumption of constant growth factor might be a reasonable approximation.

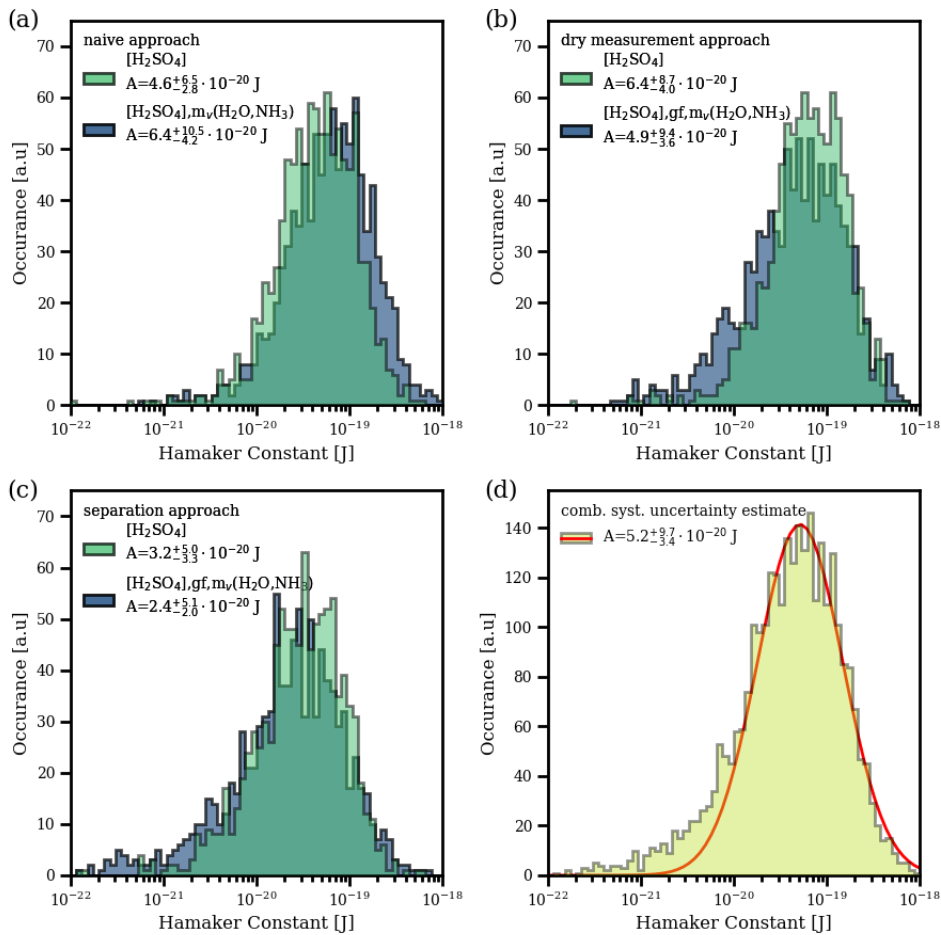


Figure S5: Systematic uncertainty estimate. Main systematic uncertainties might be related to the assumed properties of the condensing cluster, the hydration state of the measured particles and the sulphuric acid measurement. We explore the wide range of systematic uncertainties, by running the fitting algorithm 1000 times for each hygroscopicity approach, randomly assigning different parameters. The systematic uncertainty of the sulphuric acid concentrations is estimated by assigning a multiplicative offset to all sulphuric acid measurements, following a lognormal distribution with median 1 and shape parameter $\sigma_g=0.5/3$. This assures that with 99.7% probability the resulting systematic sulphuric acid offset is within the interval of +50/-33 %, which represents the maximum systematic uncertainty in the absolute sulphuric acid calibration (Kürten et al., 2012). Considering only the sulphuric acid uncertainty, the distributions of the resulting Hamaker constants are shown as the light green histograms for the three different approaches in panels (a)-(c), with the medians being identical to the results in Fig. 4b. The light purple histograms additionally consider uncertainties due to hygroscopicity and ammonia in panels (a)-(c). With equal probability, we either use 1 or 2 water molecules as assumed degree of hydration for the condensing cluster. With equal probability, we also assume that either 0 or 1 ammonia molecules condense with a sulphuric acid monomer. For the dry measurement approach, we assume a Gaussian distribution of the hygroscopic growth factor with sigma 0.1 and mean 1.25. For the separation approach, we assume an additive offset to the mass fraction of sulphuric acid and ammonia of the MABNAG prediction with sigma 0.1 and mean 0. The median of the distributions is shifted for all three approaches when all uncertainties are considered and the width of the distribution increases to some extent. Assuming an alternative description of the solution density (Hyvärinen et al., 2005) and the vapour diffusion coefficient (Cox and Chapman, 2001) resulted in a negligible impact compared to the other factors. Panel (d) shows the sum of the three approaches if all above-mentioned uncertainties are considered. They all overlap largely in the region above 10^{-20} J and fit a lognormal distribution to it, finding a best average estimate of $A = 5.2^{+9.7}_{-3.4} \cdot 10^{-20}$. Note that, all the estimates are based on the Brownian coagulation model and the results of the Hamaker constant are systematically higher if the ballistic approach is used.

Property	Approach	293.15 K 60% RH	278.15 K 60% RH	278.15 K 38% RH	Instr. cond. (DMA-train)
m_v condensing vapour mass	naïve	134 amu	134 amu	134 amu	-
	dry measurement	98 amu	98 amu	98 amu	-
	separation	98 amu	98 amu	98 amu	-
d_v hyd. vapour diameter	all	0.636 nm	0.634 nm	0.635 nm	-
ρ_v vapour density	all	1649 kg m ⁻³	1661 kg m ⁻³	1661 kg m ⁻³	-
D_v vapour diffusivity	all	$9.44 \cdot 10^{-6} \text{ m}^2 \text{ s}^{-1}$	$8.61 \cdot 10^{-6} \text{ m}^2 \text{ s}^{-1}$	$8.65 \cdot 10^{-6} \text{ m}^2 \text{ s}^{-1}$	-
l_v vapour dipole moment	all	2.84 Debye	2.84 Debye	2.84 Debye	-
α_v vapour polarizability	all	6.2 Å ³	6.2 Å ³	6.2 Å ³	-
ϵ_v vapour permittivity	all	1	1	1	-
$w(d_p, RH, T)$ particle non-water mass fraction	naïve	0.73	0.73	0.73	0.73
	dry measurement	~0.62 (not directly used)	~0.62 (not directly used)	~0.62 (not directly used)	1
	separation	0.27-0.66	0.27-0.66	0.38-0.83	0.68-0.98
$\rho_p(d_p)$ particle density	naïve	1647 kg m ⁻³	1660 kg m ⁻³	1660 kg m ⁻³	1647 kg m ⁻³
	dry measurement	1533 kg m ⁻³	1533 kg m ⁻³	1533 kg m ⁻³	1860 kg m ⁻³
	separation	1194-1566 kg m ⁻³	1204-1578 kg m ⁻³	1297-1776 kg m ⁻³	1589-1844 kg m ⁻³
$gf(d_p)$ particle growth factor	naïve	1	1	1	-
	dry measurement	1.25	1.25	1.25	-
	separation	1.50-1.21	1.51-1.20	1.30-1.07	-
ϵ_p particle permittivity	all	~100	~100	~100	-

Table S1: Used parameters. Summary of the relevant parameters, for the calculation of the theoretical collision kernels and growth rate estimates for the three different chamber conditions investigated in this study. If the assumptions are different for the different approaches on hygroscopicity, they are listed separately. The last column represents the instrument condition of the DMA-train, where particles are dried to below 5 % relative humidity. If a parameter depends on the particle size d_p , its variation between 1.5 and 7.7 nm is given (DMA-train size range in mass diameter). The densities are calculated using the parametrization of Myhre et al. (1998) for sulphuric acid water solutions. The hydrated vapour diameter is calculated from the hydrated mass (i.e. 134 amu for all approaches) and the corresponding density. The vapour diffusion coefficient is calculated using the parametrization of Hanson and Eisele (2000).

Supplementary References

- Biskos, G., Buseck, P. R. and Martin, S. T.: Hygroscopic growth of nucleation-mode acidic sulfate particles, *J. Aerosol Sci.*, 40(4), 338–347, doi:<https://doi.org/10.1016/j.jaerosci.2008.12.003>, 2009.
- Cox, K. R. and Chapman, W. G.: *The Properties of Gases and Liquids*, 5th ed., edited by B. E. Poling, J. M. Prausnitz, and J. P. O'Connell, McGraw-Hill, New York., 2001.
- Ehrhart, S., Ickes, L., Almeida, J., Amorim, A., Barmet, P., Bianchi, F., Dommen, J., Dunne, E. M., Duplissy, J., Franchin, A., Kangasluoma, J., Kirkby, J., Kürten, A., Kupc, A., Lehtipalo, K., Nieminen, T., Riccobono, F., Rondo, L., Schobesberger, S., Steiner, G., Tomé, A., Wimmer, D., Baltensperger, U., Wagner, P. E. and Curtius, J.: Comparison of the SAWNUC model with CLOUD measurements of sulphuric acid-water nucleation, *J. Geophys. Res.-Atmos.*, 121(20), 12,401–12,414, doi:[10.1002/2015JD023723](https://doi.org/10.1002/2015JD023723), 2016.
- Hanson, D. R. and Eisele, F.: Diffusion of H₂SO₄ in Humidified Nitrogen: Hydrated H₂SO₄, *J. Phys. Chem. A*, 104(8), 1715–1719, doi:[10.1021/jp993622j](https://doi.org/10.1021/jp993622j), 2000.
- Hyvärinen, A.-P., Raatikainen, T., Laaksonen, A., Viisanen, Y. and Lihavainen, H.: Surface tensions and densities of H₂SO₄ + NH₃ + water solutions, *Geophys. Res. Lett.*, 32(16), L16806, doi:[10.1029/2005GL023268](https://doi.org/10.1029/2005GL023268), 2005.
- Kürten, A.: New particle formation from sulfuric acid and ammonia: nucleation and growth model based on thermodynamics derived from CLOUD measurements for a wide range of conditions, *Atmos. Chem. Phys.*, 19(7), 5033–5050, doi:[10.5194/acp-19-5033-2019](https://doi.org/10.5194/acp-19-5033-2019), 2019.
- Lehtipalo, K., Rondo, L., Kontkanen, J., Schobesberger, S., Jokinen, T., Sarnela, N., Kürten, A., Ehrhart, S., Franchin, A., Nieminen, T., Riccobono, F., Sipilä, M., Yli-Juuti, T., Duplissy, J., Adamov, A., Ahlm, L., Almeida, J., Amorim, A., Bianchi, F., Breitenlechner, M., Dommen, J., Downard, A. J., Dunne, E. M., Flagan, R. C., Guida, R., Hakala, J., Hansel, A., Jud, W., Kangasluoma, J., Kerminen, V.-M., Keskinen, H., Kim, J., Kirkby, J., Kupc, A., Kupiainen-Määttä, O., Laaksonen, A., Lawler, M. J., Leiminger, M., Mathot, S., Olenius, T., Ortega, I. K., Onnela, A., Petäjä, T., Praplan, A., Rissanen, M. P., Ruuskanen, T., Santos, F. D., Schallhart, S., Schnitzhofer, R., Simon, M., Smith, J. N., Tröstl, J., Tsagkogeorgas, G., Tomé, A., Vaattovaara, P., Vehkamäki, H., Vrtala, A. E., Wagner, P. E., Williamson, C., Wimmer, D., Winkler, P. M., Virtanen, A., Donahue, N. M., Carslaw, K. S., Baltensperger, U., Riipinen, I., Curtius, J., Worsnop, D. R. and Kulmala, M.: The effect of acid–base clustering and ions on the growth of atmospheric nano-particles, *Nat. Commun.*, 7, 11594, doi:[10.1038/ncomms11594](https://doi.org/10.1038/ncomms11594), 2016.
- Myhre, C. E. L., Nielsen, C. J. and Saastad, O. W.: Density and Surface Tension of Aqueous H₂SO₄ at Low Temperature, *J. Chem. Eng. Data*, 43(4), 617–622, doi:[10.1021/je980013g](https://doi.org/10.1021/je980013g), 1998.